Int. J. Solids Structures Vol. 27, No. 6, pp. 681–698, 1991
Printed in Great Britain.

0020-7683/91 $3.00 + .00

COMPLIANCE OF COATED ELASTIC BODIES IN CONTACT

L. M. KEER, S. H. KIM, A. W. EBERHARDT and V. VITHOONTIEN
Department of Mechanical Engineering, Northwestern University, 2145 Sheridan Road, Evanston, IL 60208, U.S.A.

(*Received* 6 *July* 1989; *in revised form* 21 *February* 1990)

Abstract—A model is constructed to analyze the effects of normal and tangential loading on elastically identical coated spheres. The solution for a tangential displacement applied to a circular patch on the coated surfaces, including the occurrence of micro-slip (either full or partial slippage), is derived. If it is assumed that the slip region is a circular annulus of inner radius c, then the following two sets of approximations can be made: a "stiff" approximation that satisfies the zero micro-slip condition exactly for the inner circle and a "soft" approximation that satisfies the Amontons–Coulomb frictional law exactly for the slip region. It is concluded that the "soft" approximation gives an accurate value for the symmetric traction component, $\frac{1}{2}[\tau_{xz}^{(1)} - \tau_{xz}^{(2)}]$, induced by the normal and tangential loads.

1. INTRODUCTION

For many tribological applications, coated materials provide increased wear resistance. Some relevant examples of coated products are cemented carbide cutting tips (TiN, TiC), ball bearings, gears, high speed drills, milling cutters and many machine elements. In this study, the normal and sliding indentation of identical elastic spheres coated with an elastic layer is considered.

The state of stress that arises when two deformable bodies are pressed together by forces normal to the common tangent plane at the point of initial contact is of great technological interest and has a long history of study. In 1882, Hertz analyzed the problem of normal frictionless contact for isotropic, smooth homogeneous materials. Later, Cattaneo (1938) and Mindlin (1949) treated the same case for rough bodies undergoing normal and tangential loading. In the context of integral transforms, Muki (1960) has solved problems of asymmetric surface loading of an elastic half space and layer. Lysmer and Duncan (1972) published an extensive survey of literature on the problem of a uniform normal traction distributed over a circular surface region. Goodman and Keer (1975) studied the case in which the deformation takes place in identical elastic surface layers (one in each of the solids) of arbitrary thickness, bonded to a rigid substrate. In this analysis, their reasoning is extended to the case in which the substrate is elastic rather than rigid. The solution for a tangential displacement applied to a circular patch on the layer surface including the case of micro-slip (either full or partial slippage) is developed. As in the case of Goodman and Keer, it is assumed that the slip region is a circular annulus of inner radius c, and the problem is analyzed using the following two approximations: a "stiff" approximation that satisfies the zero micro-slip condition exactly for the inner circle and a "soft" approximation that satisfies the Amontons–Coulomb frictional law exactly for the slip region. Two important cases are examined. The case of a soft layer on a rigid base, as in Goodman and Keer, may be used as a model for cartilage on bone in bioengineering studies. The case of a stiff layer on a softer base, i.e., tungsten on steel, is important in tribological applications.

2. NORMAL LOADING OF COATED SPHERES

Basic equations and derivations

Suppose that two identical spheres with identical elastic surface layers are subjected to a normal force, P_z, which produces a contact area of radius a which is assumed to be small compared with the radii of the spheres, R. The geometry and coordinate system are shown in Fig. 1, along with a tangent force, P_x (see Section 3). The state of stress in each elastic

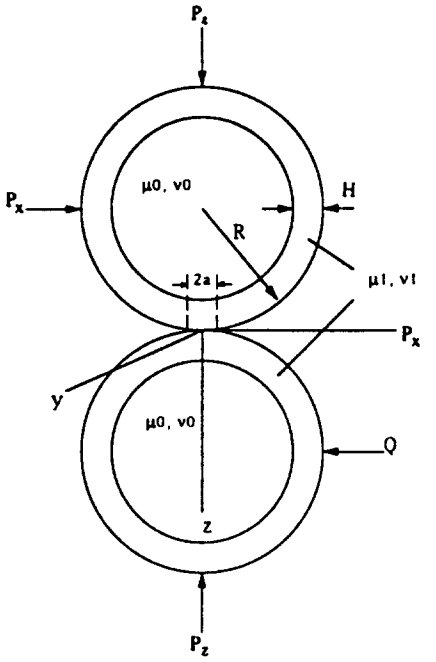

Fig. 1. Normal and tangential contact of spheres coated with an adherent layer.

layer and substrate due to the normal loading is governed by the following boundary conditions:

On $z = 0$

$$\tau_{zr1} = \tau_{z\theta 1} = 0, \quad 0 < r < \infty \tag{1a}$$

$$u_{z1} = w(r), \quad 0 < r < a \tag{1b}$$

$$\tau_{zz1} = 0, \quad a < r < \infty \tag{1c}$$

On $z = H$

$$u_{r1} = u_{r0}, \quad u_{\theta 1} = u_{\theta 0}, \quad u_{z1} = u_{z0}, \quad 0 < r < \infty \tag{2a,b,c}$$

$$\tau_{zz1} = \tau_{zz0}, \quad \tau_{zx1} = \tau_{zx0}, \quad \tau_{zy1} = \tau_{zy0}, \quad 0 < r < \infty. \tag{2d,e,f}$$

Here, subscripts 1 and 0 represent the layer and substrate, respectively.

Following Green and Zerna (1954), to satisfy the field equations of the linear theory of elasticity, displacements and stresses for elastic layer and substrate are expressed in terms of harmonic functions $F_s(r, \theta, z)$ and $G_s(r, \theta, z)$ through the relations

$$2\mu_s u_{rs} = \frac{\partial F_s}{\partial r} + z\frac{\partial G_s}{\partial r} \tag{3a}$$

$$2\mu_s u_{\theta s} = \frac{1}{r}\frac{\partial F_s}{\partial \theta} + \frac{z}{r}\frac{\partial G_s}{\partial \theta} \tag{3b}$$

$$2\mu_s u_{zs} = \frac{\partial F_s}{\partial z} - (3-4\nu_s)G_s + z\frac{\partial G_s}{\partial z} \tag{3c}$$

$$\tau_{zrs} = \frac{\partial^2 F_s}{\partial r\,\partial z} - (1-2\nu_s)\frac{\partial G_s}{\partial r} + z\frac{\partial^2 G_s}{\partial z\,\partial r} \tag{3d}$$

$$\tau_{z\theta s} = \frac{1}{r}\frac{\partial^2 F_s}{\partial \theta\,\partial z} - (1-2\nu_s)\frac{1}{r}\frac{\partial G_s}{\partial \theta} + \frac{z}{r}\frac{\partial^2 G_s}{\partial \theta\,\partial z} \tag{3e}$$

$$\tau_{zzz} = \frac{\partial^2 F_z}{\partial z^2} - 2(1-\nu_z)\frac{\partial G_z}{\partial z} + z\frac{\partial^2 G_z}{\partial z^2}, \quad (z = 0, 1). \tag{3f}$$

The harmonic functions $F_z(r, \theta, z)$ and $G_z(r, \theta, z)$ can be taken as

$$F_1(r, z) = \int_0^\infty [A \sinh(\xi z) + B \cosh(\xi z)]\xi^{-1} J_0(\xi r)\, d\xi \tag{4a}$$

$$G_1(r, z) = \int_0^\infty [C \cosh(\xi z) + D \sinh(\xi z)] J_0(\xi r)\, d\xi \tag{4b}$$

$$F_0(r, z) = -\int_0^\infty U[e^{-\xi z}]\xi^{-1} J_0(\xi r)\, d\xi \tag{4c}$$

$$G_0(r, z) = -\int_0^\infty V[e^{-\xi z}] J_0(\xi r)\, d\xi. \tag{4d}$$

The boundary conditions (1a) and (2a–f), which hold over the entire plane, are satisfied by introducing a new coefficient $\varepsilon(\xi)$ so that

$$\tau_{zz1}(r, 0) = -\int_0^\infty \varepsilon(\xi) J_0(\xi r)\xi\, d\xi. \tag{5}$$

The coefficients A, B, C, D, U and V in eqns (4a–d) can be derived by numerically solving the following simultaneous equations in terms of $\varepsilon(\xi)$:

$$\{J\}[C, D, U, V]^T = \varepsilon(\xi)\cosh\beta\,[\tanh\beta, 1, \tanh\beta, 1]^T \tag{6a,b,c,d}$$

where

$$A = (1-2\nu_1)C, \quad B = 2(1-\nu_1)D - \varepsilon(\xi) \tag{6e,f}$$

$$\{J\} = \begin{Bmatrix} \beta\sinh\beta - 2(1-\nu_1)\cosh\beta & \beta\cosh\beta - (1-2\nu_1)\sinh\beta & -\Gamma e^{-\beta} & -\Gamma\{\beta + (3-4\nu_0)\} e^{-\beta} \\ \beta\cosh\beta + (1-2\nu_1)\sinh\beta & \beta\sinh\beta + 2(1-\nu_1)\cosh\beta & \Gamma e^{-\beta} & \Gamma\beta e^{-\beta} \\ \beta\sinh\beta & \beta\cosh\beta + \sinh\beta & -e^{-\beta} & -\{\beta + (1-2\nu_0)\} e^{-\beta} \\ \beta\cosh\beta - \sinh\beta & \beta\sinh\beta & e^{-\beta} & \{\beta + 2(1-\nu_0)\} e^{-\beta} \end{Bmatrix} \tag{6g}$$

Here, $\beta = \xi H$ and $\Gamma = \mu_1/\mu_0$.

In order to satisfy boundary conditions (1b) and (1c) the following dual integral equations are developed:

$$\int_0^\infty \varepsilon(\xi) J_0(\xi r)\, d\xi - \int_0^\infty \varepsilon(\xi) L(\beta, \nu_1, \nu_0) J_0(\xi r)\, d\xi = \frac{\mu_1}{1-\nu_1} w(r), \quad 0 < r < a \tag{7a}$$

$$\int_0^\infty \varepsilon(\xi) J_0(\xi r)\xi\, d\xi = 0, \quad a < r < \infty \tag{7b}$$

with

$$L(\beta, \nu_1, \nu_0) = 1 + C(\xi). \tag{7c}$$

To solve integral equation (7a,b), a technique due to Copson (1961) is followed. When $\varepsilon(\xi)$

is expressed as

$$\varepsilon(\xi) = \xi^{1/2} \int_0^a t^{1/2} \phi_0(t) J_{-1/2}(\xi t)\, dt, \tag{8}$$

then

$$\tau_{zz1}(r,0) = \left(\frac{2}{\pi}\right)^{1/2} \left\{ -\frac{1}{(a^2-r^2)^{1/2}} \phi_0(a) + \int_r^a \frac{[\phi_0(t)]'}{(t^2-r^2)^{1/2}}\, dt \right\}, \quad 0 < r < a \tag{9a}$$

$$= 0, \quad a < r < \infty. \tag{9b}$$

Now, the boundary condition (1c) is satisfied automatically, and for the pressure vanishing at the edge of the contact region $r = a$,

$$\phi_0(a) = 0. \tag{10}$$

Following Goodman and Keer (1975), the governing equation for ϕ_0 can be derived from (7a) as

$$\phi_0(s) - s^{1/2} \int_0^a t^{1/2} \phi_0(t)\, dt \int_0^\infty L(\beta, \nu_1, \nu_0) \xi J_{-1/2}(\xi s) J_{-1/2}(\xi t)\, d\xi$$

$$= \left(\frac{2}{\pi}\right)^{1/2} \frac{\mu_1}{1-\nu_1} \frac{d}{ds} \int_0^s \frac{w(r) r}{(s^2-r^2)^{1/2}}\, dr. \tag{11}$$

The resultant normal force, P_z, is

$$P_z = \int_0^{2\pi} \int_0^a -\tau_{zz1}(r, 0, 0) r\, dr\, d\theta$$

$$= 4\left(\frac{\pi}{2}\right)^{1/2} \int_0^a \phi_0(t)\, dt. \tag{12}$$

Next, consider the two geometrically and elastically identical spheres, to which are bonded identical concentric elastic surface layers. According to Hertz theory, when these bodies are compressed by normal forces, the normal displacement at the boundary of the contact becomes

$$u_{z1}(r, 0, 0) = \tfrac{1}{2}[\delta_{ap} - r^2/R], \quad 0 < r < a \tag{13}$$

where δ_{ap} is the relative approach of the two spheres. Then, allowing $\delta_{ap} = C_1 a^2/R$, and using eqns (1b) and (13), eqn (11) becomes

$$\phi_0(s) - s^{1/2} \int_0^a t^{1/2} \phi_0(t)\, dt \int_0^\infty L(\beta, \nu_1, \nu_0) \xi J_{-1/2}(\xi s) J_{-1/2}(\xi t)\, d\xi$$

$$= \left(\frac{2}{\pi}\right)^{1/2} \frac{\mu_1}{1-\nu_1} \frac{1}{2R} (C_1 a^2 - s^2). \tag{14}$$

The stress function ϕ_0 and the relative approach term C_1 are determined simultaneously by means of solution of the symmetric Fredholm integral equation (11) and auxiliary condition (10). For an infinitely thick layer ($a/H = 0$), the Hertz result is obtained: $\delta_{ap} = a^2/R$. In general, however, $\delta_{ap} = C_1(a^2/R)$. From (10) and (11) the contact radius, a, is determined: $a/R = C_2[2(1-\nu_1)P_z/\pi a^2 \mu_1]$. From (9a), the maximum normal pressure in

Table 1. Numerical quantities for normal loading

coating layer on a rigid substrate: $\mu_1/\mu_0 = 0.0$, $\nu_1 = 0.3$;

relative approach (δ_{ap}): $\delta_{ap} = C_1 \frac{a^2}{R}$;

contact radius (a): $\frac{a}{R} = C_2\left[\frac{2(1-\nu_1)P_z}{\pi a^2 \mu_1}\right]$;

peak stress ($\tau_{zz1(max)}$): $\tau_{zz1(max)} = -C_3\left[\frac{P_z}{\pi a^2}\right]$

a/H	C_1	C_2	C_3
0.0	1.000	1.178	1.50
0.2	0.887	1.173	1.50
0.4	0.795	1.145	1.50
0.6	0.728	1.089	1.51
0.8	0.681	1.015	1.53
1.0	0.648	0.936	1.55
2.0	0.573	0.627	1.72
3.0	0.547	0.459	1.81
4.0	0.534	0.360	1.86
5.0	0.527	0.296	1.88

the contact region can be calculated: $\tau_{zz1(max)} = -C_3[P_z/\pi a^2]$. The numerical values of C_1, C_2 and C_3 are given in Tables 1 and 2 for the layer thickness range $0 < a/H < 5$, and for different layer substrate combinations.

Numerical results and discussion

Computations have been carried out for several layer substrate combinations. The thinnest layer considered had a thickness of one-fifth of the radius of the contact region. Normal stress distributions at the layer surface are given in Fig. 2. The dashed curve is the case when the substrate is rigid and corresponds to the soft coating situation studied by Goodman and Keer (1975). As was determined in their study, as the layer thickness

Table 2. Numerical quantities for normal loading

hard coating: $\mu_1/\mu_0 = 2.0$, $\nu_1 = 0.3$, $\nu_0 = 0.28$;

relative approach (δ_{ap}): $\delta_{ap} = C_1 \frac{a^2}{R}$;

contact radius (a): $\frac{a}{R} = C_2\left[\frac{2(1-\nu_1)P_z}{\pi a^2 \mu_1}\right]$;

peak stress ($\tau_{zz1(max)}$): $\tau_{zz1(max)} = -C_3\left[\frac{P_z}{\pi a^2}\right]$

a/H	C_1	C_2	C_3
0.0	1.000	1.178	1.50
0.2	1.094	1.181	1.50
0.4	1.169	1.199	1.50
0.6	1.217	1.236	1.49
0.8	1.240	1.287	1.48
1.0	1.245	1.347	1.47
2.0	1.198	1.613	1.37
3.0	1.155	1.777	1.35
4.0	1.129	1.880	1.37
5.0	1.110	1.952	1.38

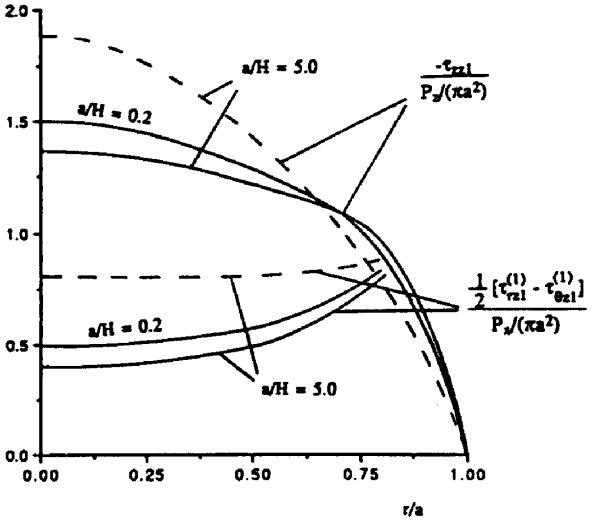

Fig. 2. Normal and shear stress distribution at surface of elastic layer without slip. (——) $\mu_1/\mu_0 = 2.0$, $\nu_1 = 0.3$, $\nu_0 = 0.28$. (— —) $\mu_1/\mu_0 = 0.0$, $\nu_1 = 0.3$.

increases the normal stress becomes less concentrated. The solid curve is the case when the layer is stiffer than the substrate. For this case the normal stress becomes more concentrated as the layer thickness increases. For $a/H = 0.2$, both cases yielded nearly identical normal stress distributions. Typical interfacial normal and shear stress distributions are given in Fig. 3 for $a/H = 1.0$. It is seen that for the same contact radius to layer thickness, a stiff layer on soft substrate (solid curve) experiences a much higher interfacial normal stress than a soft layer on a stiff base (dashed curve), while the shears are nearly the same. The peak interfacial stresses are given in Fig. 4 as a function of a/H. When the substrate is rigid (dashed curve) the interfacial normal stress becomes more concentrated as the layer thickness decreases, while the shear stress is most concentrated at $a/H \approx 1.8$. When the layer is stiffer than the substrate (solid curve), the interfacial normal stress is most concentrated at $a/H \approx 1.8$, while the maximum shear concentration occurs at $a/H \approx 3.5$.

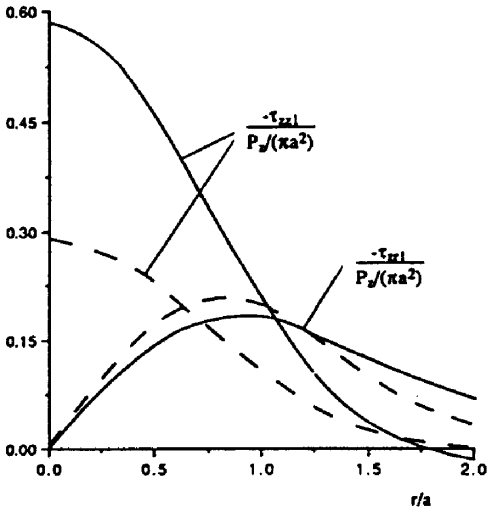

Fig. 3. Normal and shear stress distribution at the interface for normal loading ($a/H = 1$). (——) $\mu_1/\mu_0 = 2.0$, $\nu_1 = 0.3$, $\nu_0 = 0.28$. (— —) $\mu_1/\mu_0 = 0.0$, $\nu_1 = 0.3$.

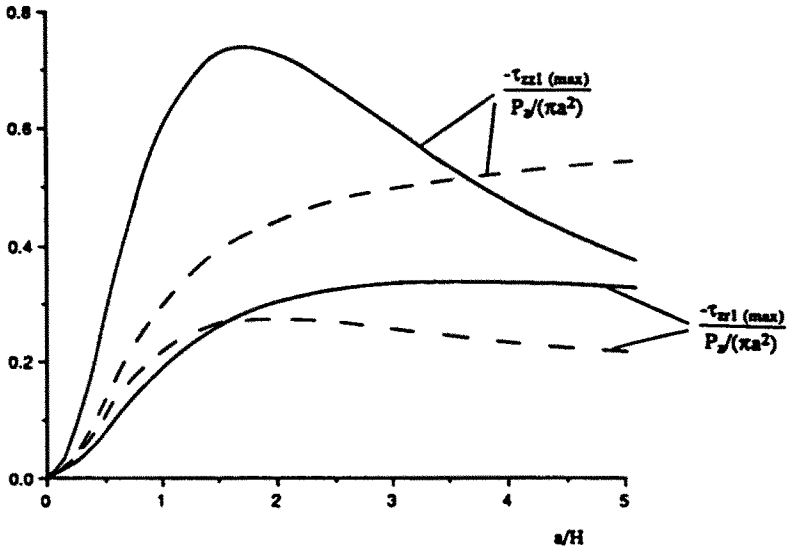

Fig. 4. Effect of layer thickness on the peak interfacial stresses for normal loading. (——) $\mu_1/\mu_0 = 2.0$, $\nu_1 = 0.3$, $\nu_0 = 0.28$. (— —) $\mu_1/\mu_0 = 0.0$, $\nu_1 = 0.3$.

3. COMPLIANCE FOR TANGENTIALLY LOADED BONDED COATED BODIES

Basic equations and derivations

Suppose now that the two elastically identical coated spheres described in the previous section are loaded in the normal direction so as to produce a contact area of radius a, assumed small compared to R, and subsequently subjected to a tangential load, P_x. The geometry and coordinate systems are shown in Fig. 1. Assuming the contact surfaces are perfectly rough, no slip will occur in the contact region. This zero-slip condition is identical to the problem of a tangential displacement applied to two welded bodies (see Goodman and Keer, 1977), provided that only those stresses arising from the relative tangential displacements are considered. The state of stress in each of the elastic layer and half space due to the addition of the tangential loading is governed by the following boundary conditions:

on $z = 0$

$$\tau_{zz1} = u_{y1} = 0, \quad u_{x1} = \Delta, \quad 0 < r < a \tag{15a}$$

$$\tau_{zz1} = \tau_{zx1} = \tau_{zy1} = 0, \quad a < r < \infty \tag{15b}$$

on $z = H$

$$u_{r1} = u_{r0}, \quad u_{\theta 1} = u_{\theta 0}, \quad u_{z1} = u_{z0}, \quad 0 < r < \infty \tag{15c}$$

$$\tau_{zz1} = \tau_{zz0}, \quad \tau_{zx1} = \tau_{zx0}, \quad \tau_{zy1} = \tau_{zy0}, \quad 0 < r < \infty. \tag{15d}$$

Here, the symbol Δ represents a uniform translational motion whose magnitude depends on P_x. To avoid additional complexity Δ is chosen such that

$$\Delta = \tfrac{1}{2}\Delta_0(r) + \Delta(r)\cos\theta. \tag{16}$$

To satisfy the field equations of the linear theory of elasticity, displacements and stresses are expressed in terms of harmonic functions $F_x(r, \theta, z)$, $G_x(r, \theta, z)$ and $H_x(r, \theta, z)$ through the relations

$$2\mu_x u_{rx} = \frac{\partial F_x}{\partial r} + z\frac{\partial G_x}{\partial r} + \frac{2}{r}\frac{\partial H_x}{\partial \theta} \tag{17a}$$

$$2\mu_\alpha u_{\theta\alpha} = \frac{1}{r}\frac{\partial F_\alpha}{\partial \theta} + \frac{z}{r}\frac{\partial G_\alpha}{\partial \theta} - 2\frac{\partial H_\alpha}{\partial r} \tag{17b}$$

$$2\mu_\alpha u_{z\alpha} = \frac{\partial F_\alpha}{\partial z} - (3-4\nu_\alpha)G_\alpha + z\frac{\partial G_\alpha}{\partial z} \tag{17c}$$

$$\tau_{zr\alpha} = \frac{\partial^2 F_\alpha}{\partial r\,\partial z} - (1-2\nu_\alpha)\frac{\partial G_\alpha}{\partial r} + z\frac{\partial^2 G_\alpha}{\partial z\,\partial r} + \frac{1}{r}\frac{\partial^2 H_\alpha}{\partial \theta\,\partial z} \tag{17d}$$

$$\tau_{z\theta\alpha} = \frac{1}{r}\frac{\partial^2 F_\alpha}{\partial \theta\,\partial z} - (1-2\nu_\alpha)\frac{1}{r}\frac{\partial G_\alpha}{\partial \theta} + \frac{z}{r}\frac{\partial^2 G_\alpha}{\partial \theta\,\partial z} - \frac{\partial^2 H_\alpha}{\partial r\,\partial z} \tag{17e}$$

$$\tau_{zz\alpha} = \frac{\partial^2 F_\alpha}{\partial z^2} - 2(1-\nu_\alpha)\frac{\partial G_\alpha}{\partial z} + z\frac{\partial^2 G_\alpha}{\partial z^2}, \quad (\alpha = 0, 1). \tag{17f}$$

Here, subscripts 1 and 0 represent the layer and half space, respectively. The harmonic functions $F_\alpha(r, \theta, z)$, $G_\alpha(r, \theta, z)$ and $H_\alpha(r, \theta, z)$ can be taken as

$$[F_\alpha(r, \theta, z), G_\alpha(r, \theta, z)]^{\mathrm{T}} = [f_\alpha(r, z), g_\alpha(r, z)]^{\mathrm{T}} \cos\theta \tag{18a}$$

$$H_\alpha(r, \theta, z) = h_\alpha(r, z)\sin\theta \tag{18b}$$

with

$$f_1(r, z) = \int_0^\infty [A\sinh(\xi z) + B\cosh(\xi z)]\xi^{-1}J_1(\xi r)\,\mathrm{d}\xi \tag{19a}$$

$$g_1(r, z) = \int_0^\infty [C\cosh(\xi z) + D\sinh(\xi z)]J_1(\xi r)\,\mathrm{d}\xi \tag{19b}$$

$$h_1(r, z) = \int_0^\infty [K\sinh(\xi z) + L\cosh(\xi z)]\xi^{-1}J_1(\xi r)\,\mathrm{d}\xi \tag{19c}$$

$$f_0(r, z) = -\int_0^\infty U[\mathrm{e}^{-\xi z}]\xi^{-1}J_1(\xi r)\,\mathrm{d}\xi \tag{19d}$$

$$g_0(r, z) = -\int_0^\infty V[\mathrm{e}^{-\xi z}]J_1(\xi r)\,\mathrm{d}\xi \tag{19e}$$

$$h_0(r, z) = -\int_0^\infty W[\mathrm{e}^{-\xi z}]\xi^{-1}J_1(\xi r)\,\mathrm{d}\xi. \tag{19f}$$

It is convenient to re-write the boundary conditions (15a–d) in cylindrical polar coordinates. With

$$[u_{r\alpha}, u_{z\alpha}, \tau_{zr\alpha}, \tau_{zz\alpha}]^{\mathrm{T}} = [u_{r\alpha}^{(1)}, u_{z\alpha}^{(1)}, \tau_{zr\alpha}^{(1)}, \tau_{zz\alpha}^{(1)}]^{\mathrm{T}}\cos\theta \tag{20a}$$

$$[u_{\theta\alpha}, \tau_{z\theta\alpha}]^{\mathrm{T}} = [u_{\theta\alpha}^{(1)}, \tau_{z\theta\alpha}^{(1)}]^{\mathrm{T}}\sin\theta, \quad (\alpha = 0, 1) \tag{20b}$$

the boundary conditions (15) and (16) may be written as

on $z = 0$

$$u_{r1}^{(1)} + u_{\theta 1}^{(1)} = 0, \quad 0 < r < a \tag{21a}$$

$$u_{r1}^{(1)} - u_{\theta 1}^{(1)} = 2\Delta, \quad 0 < r < a \tag{21b}$$

$$\tau_{zr1}^{(1)} \pm \tau_{z\theta 1}^{(1)} = 0, \quad a < r < \infty \tag{21c,d}$$

$$\tau_{zz1}(r, \theta, 0) = 0, \quad 0 < r < \infty \tag{21e}$$

on $z = H$

$$u_{z1}^{(1)} = u_{z0}^{(1)}, \quad 0 < r < \infty \tag{22a}$$

$$u_{r1}^{(1)} \pm u_{\theta 1}^{(1)} = u_{r0}^{(1)} \pm u_{\theta 0}^{(1)}, \quad 0 < r < \infty \tag{22b,c}$$

$$\tau_{zr1}^{(1)} \pm \tau_{z\theta 1}^{(1)} = \tau_{zr0}^{(1)} \pm \tau_{z\theta 0}^{(1)}, \quad 0 < r < \infty \tag{22d,e}$$

$$\tau_{zz1}^{(1)} = \tau_{zz0}^{(1)}, \quad 0 < r < \infty. \tag{22f}$$

The boundary conditions (21e) and (22), each of which holds over the entire plane, are satisfied by solving the following simultaneous equations in terms of two coefficients $S(\xi)$ and $T(\xi)$:

$$\{J\}[C, D, U, V]^{\mathrm{T}} = \tfrac{1}{2}(S-T)\cosh\beta\,[1, \tanh\beta, 1, \tanh\beta]^{\mathrm{T}} \tag{23a,b,c,d}$$

where

$$A = (1-2\nu_1)C - \tfrac{1}{2}(S-T), \quad B = 2(1-\nu_1)D \tag{23e,f}$$

$$K = \tfrac{1}{2}(S+T), \quad L = -\frac{1}{2}\frac{(S+T)(\sinh\beta+\Gamma\cosh\beta)}{\cosh\beta+\Gamma\sinh\beta}, \quad W = \frac{1}{2}\frac{(S+T)}{\cosh\beta+\Gamma\sinh\beta}e^{\beta}. \tag{23g,h,i}$$

Here $\beta = \xi H$, $\Gamma = \mu_1/\mu_0$ as before. It is interesting to note that $\{J\}$ for the tangential load is identical to $\{J\}$ for the normal load; however, the right-hand sides of the equations are different. The mixed boundary conditions (21a–d) require that

in $a < r < \infty$

$$[\tau_{zr1}^{(1)}(r,0) + \tau_{z\theta 1}^{(1)}(r,0)] = \int_0^{\infty} S(\xi)\xi J_2(\xi r)\,\mathrm{d}\xi = 0 \tag{24a}$$

$$[\tau_{zr1}^{(1)}(r,0) - \tau_{z\theta 1}^{(1)}(r,0)] = \int_0^{\infty} T(\xi)\xi J_0(\xi r)\,\mathrm{d}\xi = 0 \tag{24b}$$

in $0 < r < a$

$$2\mu_1[u_{r1}^{(1)}(r,0) + u_{\theta 1}^{(1)}(r,0)] = \int_0^{\infty} [-\nu_1 T - (2-\nu_1)S]J_2(\xi r)\,\mathrm{d}\xi + \frac{1}{2}\int_0^{\infty} [(M-N)T - (M+N)S]J_2(\xi r)\,\mathrm{d}\xi = 0 \tag{25a}$$

$$2\mu_1[u_{r1}^{(1)}(r,0) - u_{\theta 1}^{(1)}(r,0)] = \int_0^{\infty} [-\nu_1 S - (2-\nu_1)T]J_0(\xi r)\,\mathrm{d}\xi + \frac{1}{2}\int_0^{\infty} [(M-N)S - (M+N)T]J_0(\xi r)\,\mathrm{d}\xi = 4\mu_1\Delta \tag{25b}$$

where

$$M(\beta) = 2(1-\nu_1)(D-1), \quad N(\beta) = -2\left\{1 - \frac{\Gamma\cosh\beta+\sinh\beta}{\Gamma\sinh\beta+\cosh\beta}\right\}. \tag{26a,b}$$

The mixed boundary conditions are satisfied (see Westmann, 1963) by taking

$$S = \xi^{1/2} \int_0^a t^{1/2} \psi_1(t) J_{3/2}(\xi t)\, dt \tag{27a}$$

$$T = \xi^{1/2} \int_0^a t^{1/2} \chi_1(t) J_{-1/2}(\xi t)\, dt - \frac{\nu_1}{2-\nu_1} \xi^{1/2} \int_0^a t^{1/2} \psi_1(t) J_{3/2}(\xi t)\, dt. \tag{27b}$$

The resultant tangential loading is given by the expression

$$P_x = -\int_0^{2\pi} \int_0^a -\tau_{zx1}(r, \theta, 0) r\, dr\, d\theta = -\pi \int_0^a [\tau_{zr1}^{(1)}(r, 0) - \tau_{z\theta 1}^{(1)}(r, 0)] r\, dr \tag{28a}$$

$$= -(2\pi)^{1/2} \int_0^a \chi_1(t)\, dt. \tag{28b}$$

Then, using the following dimensionless forms

$$s = \sigma a, \quad t = \tau a, \quad r = \rho a, \quad \beta = \xi H,$$
$$\chi_1(s) = \mu_1 a X_1(\sigma), \quad \psi_1(s) = \mu_1 a \Psi_1(\sigma), \quad \phi_0(s) = \mu_1 a \Phi_0(\sigma), \tag{29}$$

the governing equations for Ψ_1 and X_1 can be derived from the boundary conditions (25a,b) as

$$(2-\nu_1) X_1(\sigma) + \frac{1}{\pi}\left(\frac{a}{H}\right) \int_0^1 X_1(\tau) I_5(\sigma, \tau)\, d\tau - \frac{2}{\pi} \frac{1}{2-\nu_1} \left(\frac{a}{H}\right) \int_0^1 \Psi_1(\tau) I_6(\sigma, \tau)\, d\tau$$
$$= -4\left(\frac{2}{\pi}\right)^{1/2} \frac{\Delta}{a} \tag{30}$$

and

$$\nu_1 X_1(\sigma) - \nu_1 \sigma^{-1} \int_0^\sigma X_1(\tau)\, d\tau + \frac{1}{\pi}\left(\frac{a}{H}\right) \int_0^1 X_1(\tau) I_7(\sigma, \tau)\, d\tau$$
$$- \frac{4(1-\nu_1)}{2-\nu_1} \Psi_1(\sigma) - \frac{2}{\pi} \frac{1}{2-\nu_1} \left(\frac{a}{H}\right) \int_0^1 \Psi_1(\tau) I_8(\sigma, \tau)\, d\tau = 0, \tag{31}$$

where

$$I_5(\sigma, \tau) = \int_0^\infty (M+N) \cos\left(\beta\sigma \frac{a}{H}\right) \cos\left(\beta\tau \frac{a}{H}\right) d\beta \tag{32a}$$

$$I_6(\sigma, \tau) = \int_0^\infty [M-(1-\nu_1)N] \cos\left(\beta\sigma \frac{a}{H}\right) \left[-\cos\left(\beta\tau \frac{a}{H}\right) + \left(\beta\tau \frac{a}{H}\right)^{-1} \sin\left(\beta\tau \frac{a}{H}\right)\right] d\beta \tag{32b}$$

$$I_7(\sigma, \tau) = \int_0^\infty (M-N) \left[-\cos\left(\beta\sigma \frac{a}{H}\right) + \left(\beta\sigma \frac{a}{H}\right)^{-1} \sin\left(\beta\sigma \frac{a}{H}\right)\right] \cos\left(\beta\tau \frac{a}{H}\right) d\beta \tag{32c}$$

$$I_8(\sigma, \tau) = \int_0^\infty [M+(1-\nu_1)N] \left[-\cos\left(\beta\sigma \frac{a}{H}\right) + \left(\beta\sigma \frac{a}{H}\right)^{-1} \sin\left(\beta\sigma \frac{a}{H}\right)\right]$$
$$\times \left[-\cos\left(\beta\tau \frac{a}{H}\right) + \left(\beta\tau \frac{a}{H}\right)^{-1} \sin\left(\beta\tau \frac{a}{H}\right)\right] d\beta. \tag{32d}$$

The resultant dimensionless tangential load and shear stress components on the loaded surface are obtained as

$$\frac{P_x}{\mu_1 a^2} = -(2\pi)^{1/2}\int_0^1 X_1(\tau)\,d\tau \tag{33}$$

$$\mu_1^{-1}[\tau_{zr}^{(1)}+\tau_{z\theta}^{(1)}] = \left(\frac{2}{\pi}\right)^{1/2}\left[\frac{\rho^2\Psi_1(1)}{(1-\rho^2)^{1/2}} - \rho^2\int_\rho^1 \frac{[\tau^{-2}\Psi_1(\tau)]'}{(\tau^2-\rho^2)^{1/2}}\,d\tau\right] \tag{34a}$$

$$\mu_1^{-1}[\tau_{zr}^{(1)}-\tau_{z\theta}^{(1)}] = \left(\frac{2}{\pi}\right)^{1/2}\left[(1-\rho^2)^{-1/2}\left\{X_1(1)+\frac{\nu_1}{2-\nu_1}\Psi_1(1)\right\}\right.$$
$$\left. -\int_\rho^1 \frac{X_1'(\tau)}{(\tau^2-\rho^2)^{1/2}}\,d\tau - \frac{\nu_1}{2-\nu_1}\int_\rho^1 \frac{\tau^{-1}[\tau\Psi_1(\tau)]'}{(\tau^2-\rho^2)^{1/2}}\,d\tau\right]. \tag{34b}$$

To convert the above shear stress components from polar coordinates to Cartesian coordinates the following equations are needed:

$$\tau_{zx1}(r,\theta,z) = \tfrac{1}{2}[\tau_{zr}^{(1)}-\tau_{z\theta}^{(1)}]+\tfrac{1}{2}[\tau_{zr}^{(1)}+\tau_{z\theta}^{(1)}]\cos 2\theta \tag{35a}$$

$$\tau_{zy1}(r,\theta,z) = \tfrac{1}{2}[\tau_{zr}^{(1)}+\tau_{z\theta}^{(1)}]\sin 2\theta. \tag{35b}$$

After calculating $X_1(\sigma)$ and $\Psi_1(\tau)$ [by using the no-slip conditions corresponding to eqns (30) and (31)], the stresses and displacements can be calculated numerically using (17), (18), (19), (23) and (27).

When the layer is infinitely thick ($a/H = 0$) the compliance is

$$X_1 = -\frac{4}{2-\nu_1}\left(\frac{2}{\pi}\right)^{1/2}\frac{\Delta}{a}, \quad \Psi_1 = 0. \tag{36}$$

It is noted that there is a singularity in both $[\tau_{zr}^{(1)}-\tau_{z\theta}^{(1)}]$ and $[\tau_{zr}^{(1)}+\tau_{z\theta}^{(1)}]$ at $\rho = 1$ ($r = a$). In view of eqns (35a,b) the first term on the right-hand side of eqn (34b) has a singularity in the radially symmetric portion, whereas the first term on the right-hand side of equation (34a) has a singularity in the asymmetric portion. From (36), only the radially symmetric singularity appears when the layer is infinitely thick. However, both singularities appear when the layer has finite thickness. In some cases this non-radially symmetric singularity can be ignored in an approximate sense, which can greatly simplify the analysis (see Goodman and Keer, 1975).

The physical quantity $C_x = 2\Delta/P_x$, the initial tangential compliance, is of technological interest. The variation of this quantity for various material properties and layer thicknesses is given in Table 3. For the case of a rigid substrate the results are identical to those obtained by Goodman and Keer (1975).

Numerical results and discussion

Computations have been carried out for several layer–substrate combinations. Shear stress distributions at the layer surface are given in Fig. 2. The effect of the combination of materials and layer thickness on the shear stress distribution is similar to the normal load case. Typical interfacial normal and shear stress distributions are given in Fig. 5 for $a/H = 1.0$. It is noted that the case of the stiff layer (solid curve) gives the least concentrated interfacial stress distributions. The peak interfacial stresses are given in Fig. 6. In view of eqn (35), $\frac{1}{2}[\tau_{zr}^{(1)}-\tau_{z\theta}^{(1)}]$ is the symmetric interfacial stress component whereas $\frac{1}{2}[\tau_{zr}^{(1)}+\tau_{z\theta}^{(1)}]$ is the asymmetric interfacial stress component. Both interfacial stress components increase as the layer thickness decreases; however, the interfacial stress component, $\frac{1}{2}[\tau_{zr}^{(1)}-\tau_{z\theta}^{(1)}]$, is larger than $\frac{1}{2}[\tau_{zr}^{(1)}+\tau_{z\theta}^{(1)}]$ for the case of a rigid substrate (dashed curve), while the converse is true for the case of a stiff layer (solid curve).

Table 3. Initial compliance, $C_x = 2\Delta/P_x$ (Case 1: $\mu_1/\mu_0 = 0.0$, $\nu_1 = 0.3$; Case 2: $\mu_1/\mu_0 = 0.33$, $\nu_1 = 0.33$, $\nu_0 = 0.28$; Case 3: $\mu_1/\mu_0 = 1.0$, $\nu_1 = 0.28$, $\nu_0 = 0.28$; Case 4: $\mu_1/\mu_0 = 2.0$, $\nu_1 = 0.3$, $\nu_0 = 0.28$)

	$(2\Delta/P_x)\mu_1 a = C_x\mu_1 a$			
a/H	Case 1	Case 2	Case 3	Case 4
0.0	0.425	0.418	0.418	0.425
0.2	0.387	0.397	0.418	0.447
0.4	0.352	0.377	0.418	0.468
0.6	0.321	0.360	0.418	0.486
0.8	0.295	0.345	0.418	0.503
1.0	0.272	0.332	0.418	0.518
2.0	0.194	0.286	0.418	0.574
3.0	0.150	0.258	0.418	0.613
4.0	0.122	0.240	0.418	0.640
5.0	0.104	0.227	0.418	0.661

4. THE EFFECT OF MICRO-SLIP IN TANGENTIALLY LOADED COATED BODIES

Basic equations and derivations

In the previous section tangential loading was considered for the two identical welded and coated elastic spheres. The model of normal and tangential contact loading of elastically identical coated spheres follows the same derivations as in Goodman and Keer (1975). Because a singularity arises in the absence of slip, in reality then, for this contact problem, slip must occur. If it is assumed that the slip region is a circular annulus of inner radius $c < a$, then this inner radius can be chosen so as to eliminate the radially symmetric singularity in τ_{zr1}, produced by the first term on the right-hand side of eqn (35a). When the layer is not infinitely thick, non-radially symmetric singularities occur both in τ_{zr1} and $\tau_{z\theta 1}$. Although this layer effect presents an obstacle to solving the tangentially loaded layer contact problem, it is possible to obtain upper and lower bounds for quantities of technological interest.

The state of stress for normal loading is first derived in terms of the stress function ϕ_0. When the tangential load is applied subsequent to normal loading, the state of stress is given by the harmonic functions shown in eqns (17d–f). The contact region is then divided into two parts: an inner circle, $0 < r < c$, where no slip occurs, and an annular slip zone,

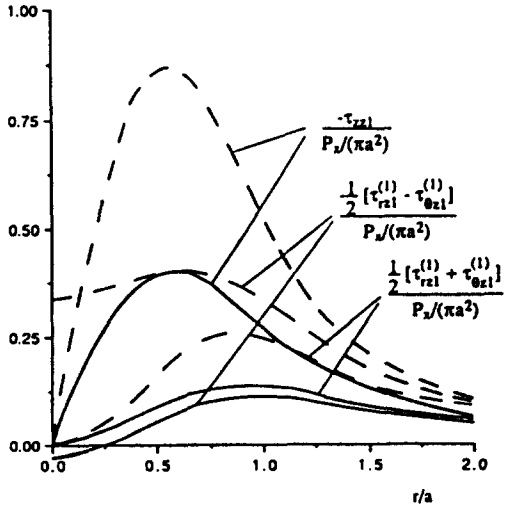

Fig. 5. Normal and shear stress distribution at the interface for tangential loading without slip ($a/H = 1$). (——) $\mu_1/\mu_0 = 2.0$, $\nu_1 = 0.3$, $\nu_0 = 0.28$. (— — —) $\mu_1/\mu_0 = 0.0$, $\nu_1 = 0.3$.

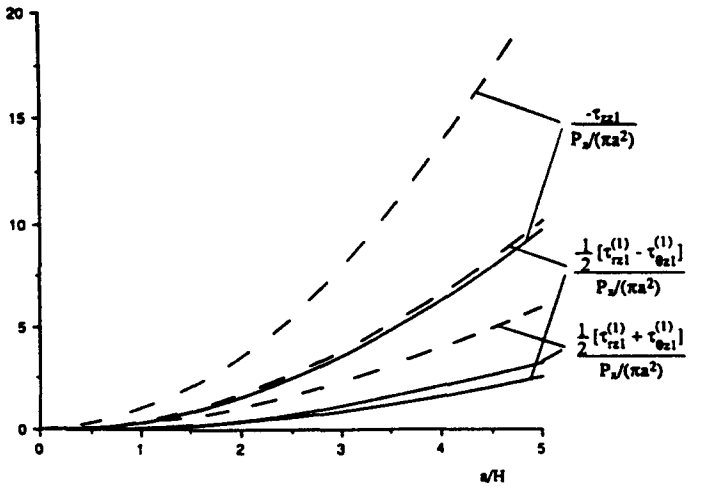

Fig. 6. Effect of layer thickness on the peak interfacial stresses for tangential loading without slip. (——) $\mu_1/\mu_0 = 2.0$, $\nu_1 = 0.3$, $\nu_0 = 0.28$. (— —) $\mu_1/\mu_0 = 0.0$, $\nu_1 = 0.3$.

$c < r < a$, where shear tractions obey the Amontons–Coulomb friction law. To satisfy these mixed boundry conditions the following equations are used instead of equations (27a,b)

$$S = \xi^{1/2}\left[\int_0^c t^{1/2}\psi_1(t)J_{3/2}(\xi t)\,dt + \frac{\delta}{a^2}\int_c^a t^{5/2}\phi_0(t)J_{3/2}(\xi t)\,dt\right] \tag{37a}$$

$$T = \xi^{1/2}\left[\int_0^c t^{1/2}\chi_1(t)J_{-1/2}(\xi t)\,dt - \frac{\nu_1}{2-\nu_1}\int_0^c t^{1/2}\psi_1(t)J_{3/2}(\xi t)\,dt\right.$$
$$\left. -2f\int_c^a t^{1/2}\phi_0(t)J_{-1/2}(\xi t)\,dt - \frac{\nu_1}{2-\nu_1}\frac{\delta}{a^2}\int_c^a t^{5/2}\phi_0(t)J_{3/2}(\xi t)\,dt\right]. \tag{37b}$$

Here, f represents the coefficient of friction and δ is, as yet, an unknown dimensionless constant that will be automatically determined later. Since there is no singularity at the boundary dividing the slip and no-slip regions, this requirement is met by imposing the auxiliary conditions

$$\chi_1(c) = -2f\phi_0(c), \quad \psi_1(c) = \delta\frac{c^2}{a^2}\phi_0(c). \tag{38a,b}$$

By substituting eqns (37) into eqn (24) and making use of eqns (29) and (38a,b), dimensionless shear stresses on the contact surface can be derived as follows:

On $z = 0$

$$\frac{1}{2\mu_1}[\tau_{z1}^{(1)} + \tau_{z0}^{(1)}] = -\frac{\rho^2}{(2\pi)^{1/2}}\left[\int_\rho^{c/a}\frac{[\tau^{-2}\Psi_1(\tau)]'}{(\tau^2-\rho^2)^{1/2}}\,d\tau\right.$$
$$\left. +\delta\int_{c/a}^1\frac{[\Phi_0(\tau)]'}{(\tau^2-\rho^2)^{1/2}}\,d\tau\right], \quad 0 < \rho < c/a \tag{39a}$$

$$= -\frac{\rho^2}{(2\pi)^{1/2}}\left[\delta\int_\rho^1\frac{[\Phi_0(\tau)]'}{(\tau^2-\rho^2)^{1/2}}\,d\tau\right], \quad c/a < \rho < 1 \tag{39b}$$

and

$$\frac{1}{2\mu_1}[\tau_{zy1}^{(1)}-\tau_{z\theta 1}^{(1)}] = -\frac{1}{(2\pi)^{1/2}}\left[\int_\rho^{c/a}\frac{X_1'(\tau)}{(\tau^2-\rho^2)^{1/2}}\,d\tau - 2f\int_{c/a}^1\frac{\Phi_0'(\tau)}{(\tau^2-\rho^2)^{1/2}}\,d\tau\right.$$
$$\left.+\frac{\nu_1}{2-\nu_1}\int_\rho^{c/a}\frac{\tau^{-1}[\tau\Psi_1(\tau)]'}{(\tau^2-\rho^2)^{1/2}}\,d\tau+\frac{\nu_1}{2-\nu_1}\delta\int_{c/a}^1\frac{\tau^{-1}[\tau^3\Phi_0(\tau)]'}{(\tau^2-\rho^2)^{1/2}}\,d\tau\right],$$
$$0<\rho<c/a \quad (39c)$$
$$=\frac{1}{(2\pi)^{1/2}}\left[2f\int_\rho^1\frac{\Phi_0'(\tau)}{(\tau^2-\rho^2)^{1/2}}\,d\tau-\frac{\nu_1}{2-\nu_1}\delta\int_\rho^1\frac{\tau^{-1}[\tau^3\Phi_0(\tau)]'}{(\tau^2-\rho^2)^{1/2}}\,d\tau\right]$$
$$c/a<\rho<\infty. \quad (39d)$$

The resultant tangential load is derived from (28a) and (39c):

$$\frac{P_x}{\mu_1 a^2} = -(2\pi)^{1/2}\left[\int_0^{c/a}X_1(\tau)\,d\tau-2f\int_{c/a}^1\Phi_0(\tau)\,d\tau\right]. \quad (40)$$

By making use of the no-slip boundary conditions, (21a,b), together with the auxiliary conditions (38a,b), governing equations for the stress functions Ψ_1 and X_1 as well as the unknown dimensionless constants f and δ can be derived in the form of the simultaneous Fredholm integral equations as

$$(2-\nu_1)X_1(\sigma)+\frac{1}{\pi}\left(\frac{a}{H}\right)\int_0^{c/a}X_1(\tau)I_5(\sigma,\tau)\,d\tau-\frac{2}{\pi}\frac{1}{2-\nu_1}\left(\frac{a}{H}\right)\int_0^{c/a}\Psi_1(\tau)I_6(\sigma,\tau)\,d\tau$$
$$=2f\frac{1}{\pi}\left(\frac{a}{H}\right)\int_{c/a}^1\Phi_0(\tau)I_5(\sigma,\tau)\,d\tau+\frac{2}{\pi}\frac{\delta}{2-\nu_1}\left(\frac{a}{H}\right)\int_{c/a}^1\Phi_0(\tau)\tau^2I_6(\sigma,\tau)\,d\tau$$
$$-4\left(\frac{2}{\pi}\right)^{1/2}\frac{\Delta}{a} \quad (41a)$$

and

$$\nu_1X_1(\sigma)-\nu_1\sigma^{-1}\int_0^\sigma X_1(\tau)\,d\tau+\frac{1}{\pi}\left(\frac{a}{H}\right)\int_0^{c/a}X_1(\tau)I_7(\sigma,\tau)\,d\tau$$
$$-\frac{4(1-\nu_1)}{2-\nu_1}\Psi_1(\sigma)-\frac{2}{\pi}\frac{1}{2-\nu_1}\left(\frac{a}{H}\right)\int_0^{c/a}\Psi_1(\tau)I_8(\sigma,\tau)\,d\tau$$
$$=2f\frac{1}{\pi}\left(\frac{a}{H}\right)\int_{c/a}^1\Phi_0(\tau)I_7(\sigma,\tau)\,d\tau+\frac{2}{\pi}\frac{\delta}{2-\nu_1}\left(\frac{a}{H}\right)\int_{c/a}^1\Phi_0(\tau)\tau^2I_8(\sigma,\tau)\,d\tau. \quad (41b)$$

The auxiliary conditions become

$$X_1\left(\frac{c}{a}\right)=-2f\Phi_0\left(\frac{c}{a}\right), \quad \Psi_1\left(\frac{c}{a}\right)=\delta\left(\frac{c}{a}\right)^2\Phi_0\left(\frac{c}{a}\right). \quad (42a,b)$$

In the slip region, $c/a<\rho<1$, shear stresses on the contact surface can be expressed [in view of (39b,d)] as

$$\tau_{zx1}=f\tau_{zz1}-\tfrac{1}{2}\rho\tau_{zz1}\delta\{e_1+\rho^2\cos 2\theta\}, \quad \tau_{zy1}=-\tfrac{1}{2}\delta\tau_{zz1}\{\rho^2\sin 2\theta\} \quad (43a,b)$$

Table 4. Bounds for tangential load, compliance and stress (stress components are evaluated at $r = 0$; $\mu_1/\mu_0 = 0.0$, $\nu_1 = 0.3$, $a/H = 5.0$)

		$\frac{c}{a} = \frac{\text{radius of non-slip region}}{\text{radius of contact region}}$			
	Bound	0.2	0.4	0.6	0.8
$\frac{P_x}{fP_z}$	A	0.994	0.946	0.794	0.475
	B	0.994	0.946	0.793	0.475
$\frac{\Delta}{P_x}\mu_1 a$	A				
	B	0.103	0.089	0.075	0.062
$\frac{1}{2}\frac{[\tau_{zr}^{(1)} - \tau_{z0}^{(1)}]}{\frac{P_x}{\pi a^2}}$	A	−1.660	−1.419	−1.182	−0.972
	B	−1.676	−1.433	−1.192	−0.977
δ/f	A	−0.202	−0.193	−0.168	−0.139

where

$$c_1 = \frac{\nu_1}{2-\nu_1}\int_\rho^1 \frac{\tau^{-1}[\tau^3\Phi_0(\tau)]'}{(\tau^2-\rho^2)^{1/2}}\,d\tau \Big/ \int_\rho^1 \frac{\Phi_0'(\tau)}{(\tau^2-\rho^2)^{1/2}}\,d\tau < 1. \tag{43c}$$

A. *Stiff approximation.* For this bound the no-slip condition (41a,b) for the circular region, $0 < \rho < c/a$, is satisfied exactly. For a given value of c/a, stress functions $X_1(\sigma)$ and $\Psi_1(\sigma)$, as well as the unknown parameters f and δ, can be determined through the use of eqns (41a,b) and (42). However, the shear stresses given in eqns (39b,d) do not satisfy the Amontons–Coulomb friction law exactly in the slip region, $c/a < \rho < 1$. The quantities in brackets in eqns (43a,b) represent error terms. This error is small, however, provided (i) a/H is small or (ii) $\delta/f < 1$. The compliance, shear stress components, P_x/fP_z and δ/f for representative values of c/a, a/H, and different layer–substrate combinations are given as bound "A" in Tables 4–6.

B. *Soft approximation.* In this bound the Amontons–Coulomb friction law is satisfied exactly at every point in the slip region, $c/a < \rho < 1$. This can be achieved by setting

Table 5. Bounds for tangential load, compliance and stress (stress components are evaluated at $r = 0$; $\mu_1/\mu_0 = 0.33$, $\nu_1 = 0.33$, $\nu_0 = 0.28$, $a/H = 5.0$)

		$\frac{c}{a} = \frac{\text{radius of non-slip region}}{\text{radius of contact region}}$			
	Bound	0.2	0.4	0.6	0.8
$\frac{P_x}{fP_z}$	A				
	B	0.993	0.942	0.790	0.480
$\frac{\Delta}{P_x}\mu_1 a$	A				
	B	0.182	0.166	0.147	0.128
$\frac{1}{2}\frac{[\tau_{zr}^{(1)} - \tau_{z0}^{(1)}]}{\frac{P_x}{\pi a^2}}$	A	−1.415	−1.173	−0.959	−0.779
	B	−1.429	−1.186	−0.967	−0.784
δ/f	A	−0.151	−0.141	−0.121	−0.099

Table 6. Bounds for tangential load, compliance and stress (stress components are evaluated at $r = 0$; $\mu_1/\mu_0 = 2.0$, $\nu_1 = 0.3$, $\nu_0 = 0.28$, $a/H = 5.0$)

		$\frac{c}{a} = \frac{\text{radius of non-slip region}}{\text{radius of contact region}}$			
	Bound	0.2	0.4	0.6	0.8
$\frac{P_x}{fP_z}$	A				
	B	0.991	0.931	0.779	0.497
$\frac{\Delta}{P_x}\mu_1 a$	A				
	B	0.451	0.423	0.391	0.359
$\frac{1}{2}\frac{[\tau_{zr}^{(1)} - \tau_{z\theta}^{(1)}]}{\frac{P_x}{\pi a^2}}$	A	−1.057	−0.808	−0.629	−0.501
	B	−1.047	−0.798	−0.621	−0.495
δ/f	A	0.108	0.104	0.086	0.065

$\Psi_1(\sigma) = \delta = 0$ in eqns (43a,b). Then

$$\tau_{zz1} = -\frac{\mu_1}{(2\pi)^{1/2}}\left[\int_\rho^{c/a} \frac{X_1'(\tau)}{(\tau^2-\rho^2)^{1/2}}\,d\tau - 2f\int_{c/a}^1 \frac{\Phi_0'(\tau)}{(\tau^2-\rho^2)^{1/2}}\,d\tau\right], \quad 0 < \rho < c/a \tag{44a}$$

$$= -\frac{2\mu_1 f}{(2\pi)^{1/2}}\int_\rho^1 \frac{\Phi_0'(\tau)}{(\tau^2-\rho^2)^{1/2}}\,d\tau = f\tau_{zz1}, \quad c/a < \rho < 1 \tag{44b}$$

$$\tau_{zr1} = 0, \quad 0 < \rho < \infty. \tag{44c}$$

By making use of the no-slip conditions in the x direction (41a) together with the auxiliary condition (42a) $X_1(\sigma)$ and f can be obtained. The result of this approximation is that the boundary condition $\tau_{zr1} = 0$ is satisfied as shown in eqn (44c) instead of $u_{r1} = 0$.

The compliance, shear stress components, P_x/fP_z and δ/f for the representative values of c/a, a/H, and different layer–substrate combinations are given as bound "B" in Tables 4–6.

Numerical results and discussion

Computations have been carried out for several layer–substrate combinations. The bounds for tangential load, compliance and surface stress components are given in Tables 4–6. It is noted that, for all layer–substrate combinations considered, the tangential load and compliance were identical to three decimal points. As the layer thickness decreases (a/H increases) these combinations give different results. Typical and most sensitive of these quantities is the stress. When the layer is softer than the substrate, the "soft" approximation gives an upper bound and the "stiff" approximation gives a lower bound for the symmetric stress component. When the layer is stiffer than the substrate, on the other hand, the "soft" approximation gives a lower bound and the "stiff" approximation gives an upper bound for the symmetric stress components. This trend is reflected by the quantity μ_1/μ_0. When $\mu_1/\mu_0 > 1$, the stiff approximation yields an upper bound: when $\mu_1/\mu_0 < 1$, the soft approximation yields the upper bound. However, in each case the two approximations yield a solution which differs by less than 3%. Therefore, in the present figures, only the results using the soft approximation are shown. These trends are shown for the two cases: a coating layer on a rigid substrate (Fig. 7a) and a hard coating layer on a soft substrate (Fig. 7b).

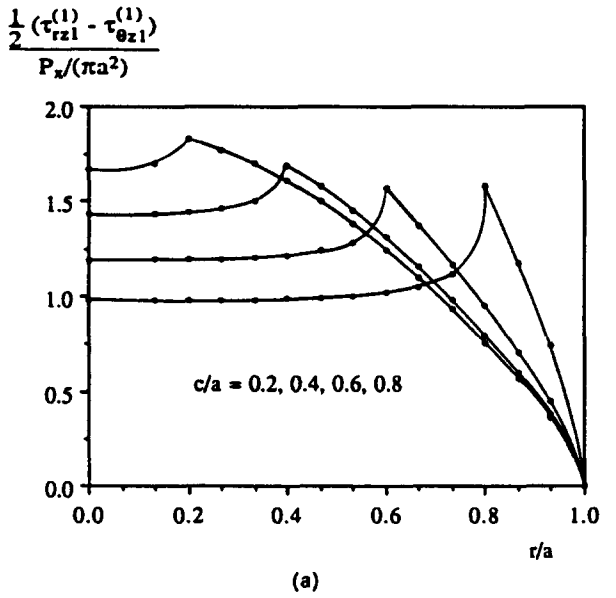

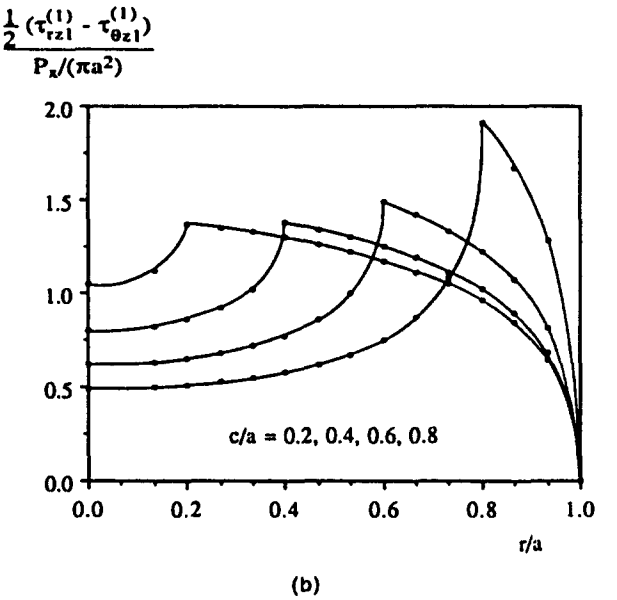

Fig. 7. (a) Shear stress distribution at surface of elastic layer with micro-slip. $a/H = 5.0$, $\mu_1/\mu_0 = 0.0$ and $\nu_1 = 0.3$. (b) Shear stress distribution at surface of elastic layer with micro-slip. $a/H = 5.0$, $\mu_1/\mu_0 = 2.0$, $\nu_1 = 0.3$, and $\nu_0 = 0.28$. c/a = radius of no-slip region/radius of contact region.

The relations between the size of slip zone, lateral motion and tangential load for those cases are presented for rigid substrate (Fig. 8a) and for a hard coating (Fig. 8b). For all cases, the thickness of the coating layer exhibits an insignificant influence on the ratio of shear traction and friction force. In other words, P_x/fP_z is independent of the layer thickness for both hard and soft coatings. On the contrary, the ratio of lateral motion in the absence of slip and lateral motion with slip, Δ_x/Δ_x, varies with the layer thickness. The type of coating (hard or soft) also has a significant influence on the lateral motion. For a soft coating, the ratio of the lateral motion increases as the coating layer becomes thicker, while the opposite conclusion is true for a hard coating. In future studies in these areas, the soft approximation should be used since it is simpler and more cost-effective with regard to computer time.

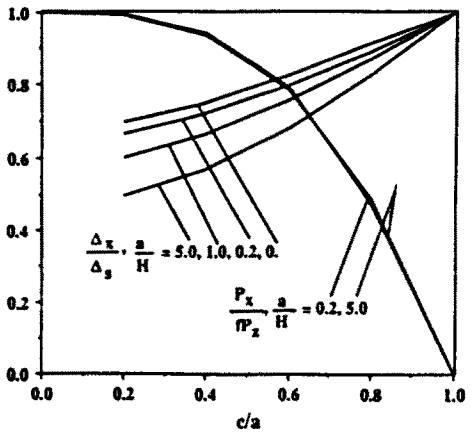

(a)

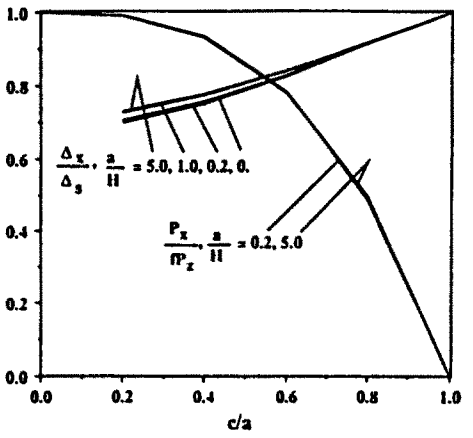

(b)

Fig. 8. (a) Relation between slip zone dimension, lateral motion and tangential load for $\mu_1/\mu_0 = 0.0$ and $\nu_1 = 0.3$. (b) Relation between slip zone dimension, lateral motion and tangential load for $\mu_1/\mu_0 = 2.0$, $\nu_1 = 0.3$ and $\nu_0 = 0.28$. a/H = radius of contact region/thickness of elastic layer; c/a = radius of no-slip region/radius of contact region; Δ_s/Δ_r = lateral motion in absence of slip/lateral motion with slip.

Acknowledgement—The authors are grateful for the support of this research by the Center for Engineering Tribology.

REFERENCES

Cattaneo, C. (1938). Sul contatto di due corpi elastici. *Acc. dei Lincei, Rend. Ser.* 6, **27**, I, 342–348; II, 434–436; III, 474–478.

Copson, E. T. (1961). On certain dual integral equations. *Proc. Glasgow Math. Assoc.* 21–24.

Goodman, L. E. and Keer, L. M. (1975). Influence of an elastic layer on the tangential compliance of bodies in contact. In *The Mechanics of the Contact Between Deformable Bodies* (Edited by A. D. de Pater and J. J. Kalker), pp. 127–151. Delft University Press.

Goodman, L. E. and Keer, L. M. (1977). Near field stress analysis of a spot weld between elastic plates. *Int. J. Solids Struct.* **13**, 151–158.

Green, A. E. and Zerna, W. (1954). *Theoretical Elasticity*, 1st Edn, pp. 169–170. Oxford University Press.

Hertz, H. (1882). Uber die Beruhrung fester elastischer Korper. *J.f.d. Reine u. Angew. Math.* **92**, 156–171.

Lysmer, J. and Duncan, J. M. (1972). *Stresses and Deflections in Foundations and Pavements*, 5th Edn. Department of Civil Engineering, University of California, Berkeley, CA.

Mindlin, R. D. (1949). Compliance of elastic bodies in contact. *J. Appl. Mech.* **16**, 259–268.

Muki, R. (1960). Asymmetric problems of the theory of elasticity for a semi-infinite solid and a thick plate. In *Progress in Solid Mechanics* (Edited by I. N. Sneddon and R. Hill), Vol. 1. North-Holland, Amsterdam.

Westmann, R. A. (1963). Simultaneous pairs of dual integral equations. *SIAM Rev.* **7**, 341–348.